

Photonic Assisted Generation of Arbitrary Millimeter-Wave and Microwave Electromagnetic Waveforms via Direct Space-to-Time Optical Pulse Shaping

Jason D. McKinney, *Member, IEEE, Member, OSA*, Dongsun Seo, Daniel E. Leaird, *Member, IEEE*, and Andrew M. Weiner, *Fellow, IEEE, Fellow, OSA*

Abstract—We present our work in optical generation of arbitrarily shaped millimeter-wave electromagnetic waveforms. Through a novel technique, which utilizes tailored optical pulse sequences from a direct space-to-time pulse shaper to drive a high-speed optical-to-electrical converter, we generate amplitude-equalized, arbitrarily phase- and frequency-modulated waveforms at center frequencies approaching 50 GHz. In addition, we demonstrate the extension of this technique to generation of arbitrary electromagnetic waveforms in the low-gigahertz range, through dispersive stretching of the pulse shaper output. In the dispersively stretched configuration, the duration of our electrical waveforms is tuned through simple alignment changes in our pulse-shaping apparatus.

Index Terms—Arbitrary waveform generation, optoelectronics, pulse shaping, radio frequency (RF) photonics, ultrafast optics.

I. INTRODUCTION

THE emerging area of microwave photonics, which exploits optical techniques to generate, measure, and transmit microwave and millimeter-wave analog data, has seen much growth over the past several years. Various methods for photonic analog-to-digital conversion have been demonstrated utilizing several optical-time-division-demultiplexing schemes [1], [2] in addition to time-stretching techniques [3] with the goal of measuring electronic signals in the microwave and millimeter-wave range. Fiber-wireless systems [4] have also been demonstrated for optical transmission of electrical signals in the millimeter-wave band. Optical generation of electromagnetic waveforms in the gigahertz and multiple-tens-of-gigahertz range, specifically arbitrarily shaped waveforms, is an area that warrants further exploration.

Manuscript received April 8, 2003; revised August 15, 2003. This work was supported in part by the U.S. Army Research Office under Contract DAAD19-00-0497, the National Science Foundation under Grant 0100949-ECS, and by Intel. The work of D. Seo was supported by the Korea Science and Engineering Foundation (under Grant R01-2000-000-00249-0) and the Integrated Photonics Technology, ERC, Inha University, Korea.

J. D. McKinney, D. E. Leaird, and A. M. Weiner are with the School of Electrical and Computer Engineering, Purdue University, West Lafayette, IN 47907-2035 USA (e-mail: mckinnjd@ecn.purdue.edu).

D. Seo is with the School of Electrical and Computer Engineering, Purdue University, West Lafayette, IN 47907 USA, on leave from the Department of Electronics, Myongji University, Yongin, Kyonggido 449-728, Korea.

Digital Object Identifier 10.1109/JLT.2003.822246

Arbitrarily shaped millimeter and microwave waveforms could find applications in a variety of radio-frequency (RF) communications systems, including ultra-wide-bandwidth (UWB) [5], secure, and multiple-access systems, in addition to other areas such as electronic countermeasures and pulsed radar. Current electromagnetic arbitrary waveform generation (AWG) technology is, however, limited to the range below ~ 2 GHz. Novel optical techniques for generation of arbitrarily shaped electromagnetic waveforms could remarkably improve the current state-of-the-art in millimeter-wave and microwave AWG. Recently, several techniques have been demonstrated for generation of narrow-band electromagnetic signals in the 1–10-GHz range. A system employing a tunable laser diode source, electrooptic modulator, and fiber delay lines has been demonstrated to produce tunable RF radiation from 550 MHz–9 GHz through RF interference [6]. In addition, a mode-locked laser diode, combined with a wavelength-division-demultiplexing technique has been demonstrated to produce narrow-band electromagnetic signals, in the 12.4–37.2-GHz range, through beating of different longitudinal laser modes. This technique also allows individual longitudinal modes of the laser to be independently phase- or amplitude-modulated, allowing arbitrarily shaped beat signals to be generated [7]. These techniques, while producing spectrally pure electromagnetic radiation, are narrow-band techniques, allowing modulation of the gigahertz waveforms over many cycles of the underlying periodic signal. Recently, a wide-band phase-modulated waveform in the low (~ 6) GHz range has been demonstrated through a wavelength-division-multiplexing (WDM) scheme combined with a series of optical delay lines used to create an optical pulse sequence to drive a photodiode [8]. This technique, while demonstrating cycle-by-cycle generation of electromagnetic waveforms, suffers from the need to tailor the fiber delay lines to each specific waveform. Consequently, reprogrammability is not easily achieved. A reprogrammable technique, based on spectral amplitude shaping of a supercontinuum source using a Fourier transform pulse-shaping technique and dispersive stretching, has also been demonstrated for generation of RF waveforms in the 1–12-GHz range [9].

In this work, we present an overview of our work in photonically assisted generation of broad-band electromagnetic

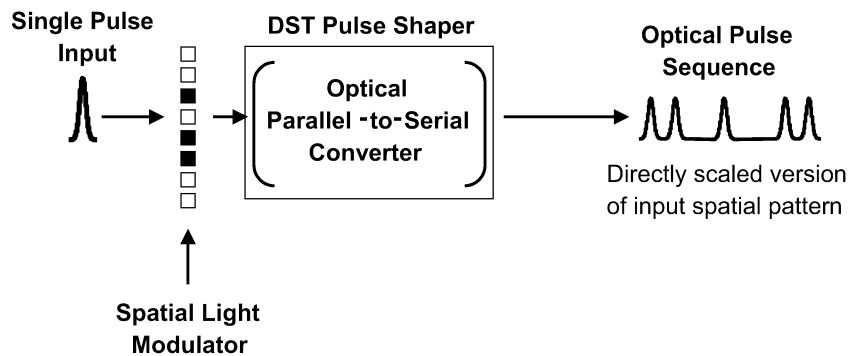


Fig. 1. Schematic operation of the DST pulse shaper. A spatially patterned short pulse input is converted to a temporal output, which is a directly scaled version of the applied spatial pattern. The DST shaper essentially performs optical parallel-to-serial conversion.

waveforms. Our technique, based on direct space-to-time (DST) optical pulse shaping [10], enables reprogrammable cycle-by-cycle generation of arbitrarily shaped phase- and frequency-modulated waveforms from ~ 2 –50 GHz. While we have demonstrated arbitrary burst [11] and continuous [12] millimeter waveform generation previously, this work represents the first all-inclusive picture of our experiments in photonically assisted millimeter-wave AWG and the extension of this technique to tunable electromagnetic waveforms in the microwave regime.

This paper is organized as follows. In Section II, we will discuss our experimental setup and the basics of the DST optical pulse shaper, which forms the basis for our millimeter-wave AWG apparatus. Section III will present a review of our broad-band burst and continuous millimeter-wave AWG results, in which we generate arbitrarily phase- and frequency-modulated waveforms in the ~ 30 –50 GHz range. Our recent experiments in moving this technique to the gigahertz range will be discussed in Section IV, and in Section V, we will conclude.

II. EXPERIMENTAL CONCEPT AND APPARATUS

Our work utilizes high-rate optical pulse sequences and high-speed optical-to-electrical (O/E) conversion to generate broad-band electrical waveforms. These high-rate optical pulse sequences are generated in a novel DST optical pulse shaper operating in the $1.55\text{-}\mu\text{m}$ optical communications wavelength band. Though not as widely known as Fourier transform (FT) pulse shaping [13], DST pulse shaping provides a simple manner by which to generate optical pulse sequences. The basic functionality of the DST shaper is illustrated in Fig. 1. In contrast to the Fourier relation between the spatial mask and temporal output in FT shaping, the output temporal waveform from a DST shaper is a directly scaled version of the spatial pattern applied to a short pulse at the input of the shaper. Functionally, the DST shaper acts as a parallel-to-serial converter for this short pulse input. Changes in the output pulse sequence are induced simply by changing the applied spatial pattern at the pulse shaper input. This straightforward relationship between the applied spatial pattern and the pulse shaper temporal output makes the system ideally suited for optical pulse sequence generation. The spatial light modulator (SLM) shown in Fig. 1 could be a fixed amplitude mask as in previous work [10], [14],

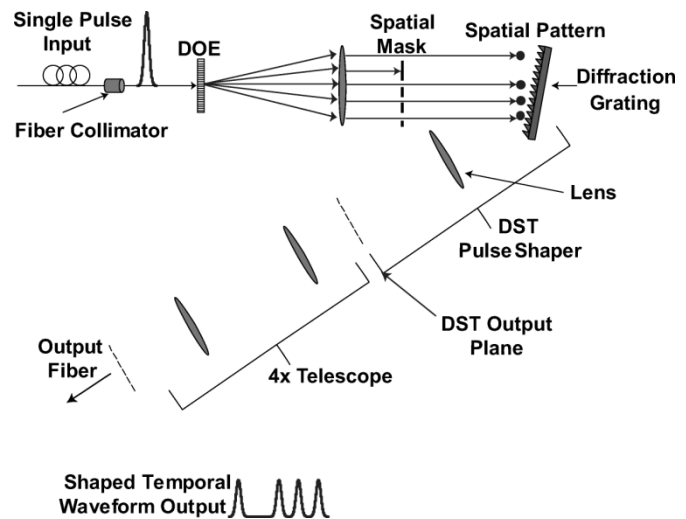


Fig. 2. Novel $1.5\text{-}\mu\text{m}$ DST optical pulse shaper. Our DST shaper enables generation of optical pulse sequences at rates of ≥ 100 GHz, which span a temporal window ≥ 100 ps.

a reprogrammable SLM (such as a liquid-crystal modulator or high-speed optoelectronic modulator array), or the combination of a diffractive optical element that generates fixed spatial patterns and an amplitude mask as demonstrated here.

Our novel pulse shaping apparatus is shown in Fig. 2. The output from one of several mode-locked fiber lasers (the specifics of which will be discussed in the following section) is collimated using a fiber-pigtailed collimating lens and forms the short pulse input to our system. This beam is spatially patterned using a diffractive optical element (DOE) (custom device, INO, QC, Canada), a phase-only mask that functions as a one-dimensional spot generator. This mask splits the single input beam into N output beams with essentially no loss. Our devices have multiple DOEs, which produce patterns ranging from 8–21 spots on a single substrate. Subsequent to the DOE, an amplitude mask is employed to further manipulate these periodic patterns by blocking individual spots. The primary application of our DST pulse shaper is generation of high-rate optical pulse sequences for optical communications applications. Looking ahead to high-speed optoelectronic modulator arrays for pattern manipulation, we have chosen to utilize the fixed periodic spatial patterns generated by DOEs. The fixed pulse timing of the periodic optical pulse sequences

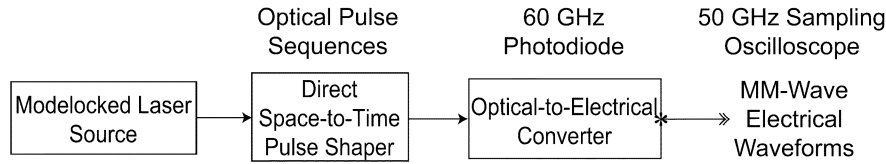


Fig. 3. Experimental schematic. Single pulses from a mode-locked laser are converted to pulse sequences in the DST shaper. These optical pulse sequences are then converted to millimeter-wave electromagnetic signals via a high-speed photodiode which are measured on a 50-GHz sampling oscilloscope.

that result from space-to-time conversion of these patterns is a necessity for high-speed optical communications applications which require minimal timing jitter in the optical bit stream. Because we have adopted our DST pulse shaper as the basis for our arbitrary electromagnetic waveform generation experiments, the correct spatial pattern (and, hence, optical pulse sequence) for the desired electrical waveform must be chosen through translation to different DOEs on the substrate. The spatial patterns generated in this manner are then used as the input to our pulse shaper, which consists of a 600-l/mm low polarization-dependent loss (PDL) telecom diffraction grating and a 15-cm achromat lens. The thin slit previously used to sample the pulse shaper output [14] has been replaced with a single-mode optical fiber. To appropriately match the pulse shaper output to the fiber mode, a $4 \times$ telescope has been placed between the DST shaper and the output fiber. Mathematically, the pulse shaper output is the convolution of the input short pulse and the applied spatial pattern, as follows:

$$E_{\text{DST}} \propto e_{\text{in}}(t) * m\left(-\frac{\alpha}{\lambda}t\right). \quad (1)$$

In this expression, $e_{\text{in}}(t)$ is the short pulse input and $m(-\alpha t/\lambda)$ is the applied spatial pattern evaluated as a function of time. The space-to-time conversion constant in picoseconds per millimeter is given by

$$\frac{\gamma}{\alpha} = \frac{\lambda}{cd \cos \theta_i} \quad (2)$$

where λ is the system center wavelength (1558 nm), c is the speed of light, d is the period of the diffraction grating (1/600 mm), and θ_i is the angle of incidence ($\sim 12^\circ$) of the input pattern on the grating. These values give a space-to-time conversion constant of ~ 3.1 ps/mm for our system. Our DOEs provide a variety of periodic spatial patterns for use as the input to our pulse shaper. These patterns, generally ~ 32 mm in length, amount to ~ 100 ps optical pulse sequences after space-to-time conversion.

The concept of our experiment is to use arbitrary optical pulse sequences generated by the DST shaper to drive a bandwidth-limited electrical system. This is shown schematically in Fig. 3. Pulses from a mode-locked laser source are converted to arbitrary optical pulse sequences in the DST shaper. These pulse sequences are then converted to millimeter electromagnetic waveforms through O/E conversion by a 60-GHz photodiode and are subsequently measured on a 50-GHz sampling oscilloscope. Here, the limited bandwidth of the electrical measurement suppresses harmonics in the optical pulse sequences—effectively converting isolated optical pulses into smooth millimeter-wave sinusoids.

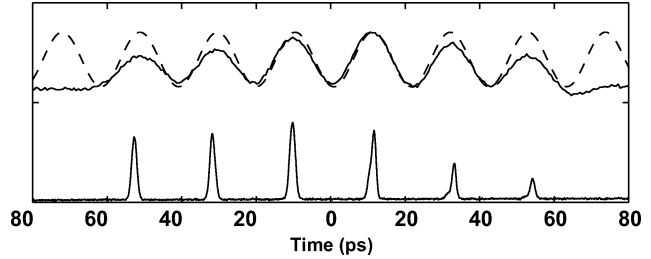


Fig. 4. Burst millimeter waveforms. By taking advantage of the limited electrical system bandwidth, pulse sequences consisting of isolated optical pulses are converted to smooth millimeter-wave sinusoids. For example, here we illustrate a ~ 48 -GHz burst millimeter waveform (solid), sinusoidal fit (dashed), and driving optical pulse sequence (bottom trace).

III. MILLIMETER-WAVE ARBITRARY WAVEFORM GENERATION

A. Broad-band Burst Millimeter Waveform Generation

Our first experiments in millimeter-wave AWG [11] involve the generation of arbitrarily shaped broad-band burst electromagnetic waveforms. In these experiments, the source laser is a passively mode-locked erbium fiber laser which provides ~ 300 fs pulses at a rate of 40 MHz. Each pulse from the source is converted to an optical pulse sequence spanning a time aperture ≥ 100 ps in the DST shaper and converted to an electromagnetic waveform by the high-speed photodiode. A ~ 48 -GHz sinusoidal burst generated in this manner is shown in Fig. 4.

Here, we have applied a series of six spots to the pulse shaper input. The spatial period of ~ 6.7 mm for this pattern yields a series of six optical pulses at the pulse shaper output with a pulse rate of ~ 48 GHz after space-to-time conversion. This sequence is then used to drive the photodiode. Comparing the optical cross correlation of the driving optical pulse sequence (bottom trace) with the measured electrical waveform, each pulse clearly contributes one cycle to the electrical waveform. This ~ 48 -GHz burst waveform is seen to be a smooth sinusoid, in stark contrast with the driving optical pulse sequence, and shows excellent agreement with a ~ 48 -GHz sinusoidal fit. Given the mapping of one optical pulse to one electrical cycle, we need only to change the period of the optical pulse sequence to alter the frequency of the electrical waveform. This is simply accomplished by changing the periodic spatial input pattern to the DST shaper.

Each cycle of the electrical waveform is generated from a single pulse from the DST shaper. This enables not only generation of periodic waveforms, but also the ability to phase- and frequency-modulate these waveforms. For example, consider the periodic waveform of Fig. 4. The six-pulse sequence forming the basis for this waveform is generated by removing every other pulse from a ~ 96 -GHz 14-pulse sequence. If the same sequence is utilized but a portion of the sequence is shifted

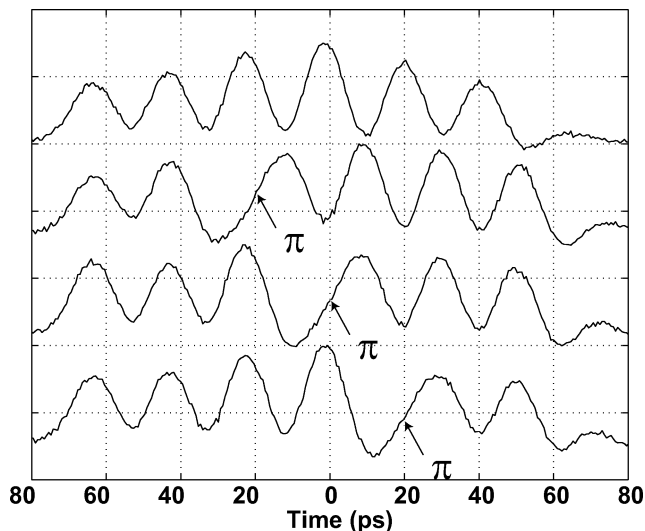


Fig. 5. ~ 48 -GHz phase modulation. The phase of the electrical waveform is controlled by altering the temporal position of pulses in the optical pulse sequence. The top trace is the ~ 48 -GHz burst waveform of Fig. 4(a). In the lower traces, a π phase shift occurs after the second, third, and fourth cycle in the electrical waveform as determined by the location of an extra 10-ps delay in the driving optical pulse sequence.

by one pulse, an extra ~ 10 -ps delay is introduced at the location of the shift. After O/E conversion, this amounts to a π phase shift at the corresponding location in the electrical waveform. Fig. 5 shows a series of three ~ 48 -GHz phase-modulated waveforms generated in this manner. In the lower three waveforms, an extra 10-ps delay is introduced after the second, third, and fourth pulse in the driving optical pulse sequence, respectively. This introduces a π phase shift after the second, third, and fourth electrical cycle as compared with the periodic ~ 48 -GHz waveform (top trace). As these waveforms illustrate, the phase of the electrical waveform is controlled by the temporal position of pulses in the driving optical pulse sequence.

If we instead wish to frequency-modulate our waveforms, we alter the spacing of pulses in the optical pulse sequence. The idea is to drive the photodiode with a pair of pulses spaced so closely they cannot be individually resolved by the electrical measurement. The result is that the electrical responses from each individual pulse in the pair blend together to produce a single electrical cycle that is twice the duration of that induced by a single pulse. This is illustrated in Fig. 6(a). Here, three pulses at ~ 48 GHz are followed by two pulse pairs, as shown in the bottom trace. The pulse-to-pulse spacing in these pairs is ~ 10 ps—too close in time for the electrical system to distinguish them. The result is an electrical waveform that exhibits three cycles at ~ 48 GHz followed by two cycles at ~ 24 GHz. This example very clearly illustrates our ability to generate millimeter waveforms in a cycle-by-cycle manner. As is evident from this waveform, when the pulse pairs are of similar amplitude to the individual pulses driving the high-frequency portion of the waveform, the lower frequency cycles are larger in amplitude. This is explained by the fact that not only does the O/E converter see twice the energy as for single pulse excitation, but the electrical system response is also greater at ~ 24 GHz than at ~ 48 GHz. To remove this distortion and obtain equalized electrical waveforms, the driving optical pulse sequence is pre-

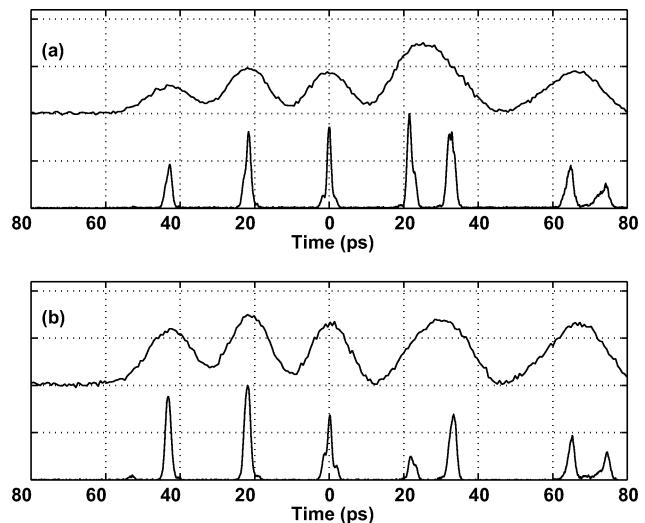


Fig. 6. Millimeter-wave frequency modulation (FM). The frequency of the electrical is mediated by the pulse spacing in the optical pulse sequence. (a) $\sim 48/24$ -GHz frequency-modulated burst waveform. Here, the pulse pairs in the driving optical pulse sequence (bottom trace) are of similar amplitude to the single pulses driving the high-frequency portion of the waveform. This leads to an amplitude difference across the measured waveform. (b) Equalized $\sim 48/24$ -GHz frequency-modulated waveform. Predistortion of the optical pulse sequence allows individual cycles of the electrical waveform to be equalized independently.

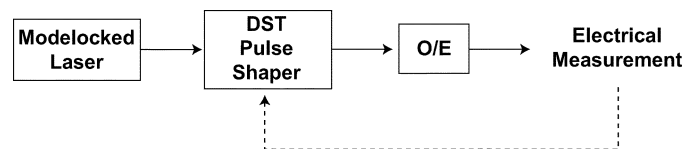


Fig. 7. Tailoring of the electrical waveform. Predistortion of the driving optical pulse sequence based on the electrical measurement allows the electrical waveforms to be shaped as desired.

distorted to decrease the amplitude of the ~ 24 -GHz cycles. The result is shown in Fig. 6(b). Comparing the electrical waveforms of Fig. 6(a) and (b), it is clear the low-frequency cycles are now of similar amplitude to the high-frequency cycles. The equalization operation is shown schematically in Fig. 7. In this manner, the shape of the electrical waveform may be tailored as desired, for example equalized, by appropriate predistortion of the driving optical pulse sequence based on the electrical measurement.

To illustrate the broad-band nature of our burst waveforms, we present RF power spectra for several of these waveforms in Fig. 8, calculated by performing a Fourier transform of the time-domain data. The spectrum for the ~ 48 -GHz sinusoidal burst of Fig. 4 is shown in (a). The spectrum is found to have a center frequency of ~ 48 GHz and a bandwidth of ~ 7 GHz, as determined by the approximately 130-ps duration of the waveform. In (b), the spectrum of the frequency-modulated waveform of Fig. 6(b) is presented. Here, the spectrum shows features at ~ 24 and ~ 48 GHz as expected and dramatically illustrates the broad bandwidth of our waveforms, with nonzero spectral content over the range of ~ 15 –60 GHz.

This illustrates our ability to generate broad-band, amplitude equalized, arbitrarily phase- and frequency-modulated waveforms in multiple-tens-of-gigahertz range through O/EI conversion of tailored optical pulse sequences.

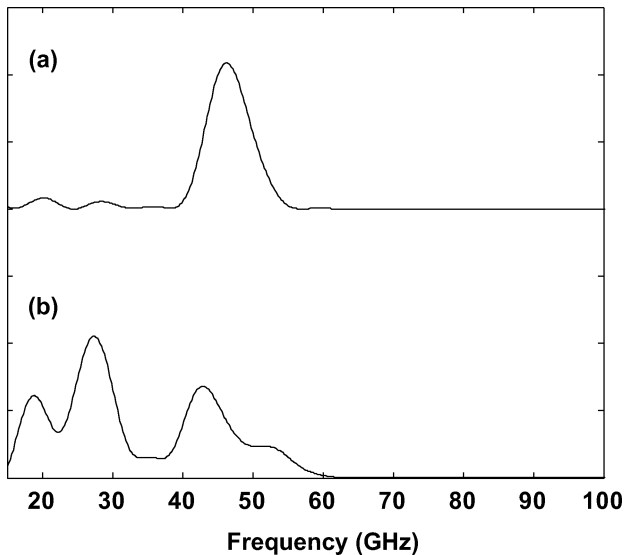


Fig. 8. Calculated RF power spectra for (a) ~ 48 -GHz sinusoidal burst and (b) $\sim 48/\sim 24$ -GHz frequency-modulated burst waveform.

In our system, the input pulse to the DST shaper is split into N pulses by the DOE, and a subsequent spatial amplitude mask is then used to tailor the desired pulse sequence. As mentioned previously, our DOEs provide periodic spatial patterns ranging from 8–21 spots. Since we are currently using a fixed mask subsequent to the DOE, the number of DOE spots must be equal to at least twice the number of pulses in the desired optical pulse sequence to allow tailoring of the spatial pattern. This amounts to spatial patterns from the DOE that yield pulse sequences at twice the desired repetition rate, e.g., a ~ 100 -GHz pulse sequence is used to generate a ~ 50 -GHz sequence through removal of every other input spot. For example, to generate the six-cycle ~ 48 -GHz waveforms of Figs. 4 and 5, a series of 20 spots formed the basis for the resulting waveforms. In terms of patterning efficiency, the electrical waveforms utilize m/N of the input optical power where m is the number of optical pulses necessary to generate the desired electrical waveform. Typically, the patterning efficiency is on the order of 50%. The efficiency of the pulse-shaping apparatus itself, which determines the optical power coupled into the output fiber of the pulse shaper, depends upon the input pulsewidth and the pulse-shaping time aperture and is thoroughly discussed in [10]. The waveforms generated in this experiment exhibit peak-to-peak amplitudes of roughly 3 mV, which is determined by the optical excitation power and the efficiency of the 60-GHz photodiode. If applications require larger amplitude signals, either increased optical excitation power or wide-band electrical amplification could be used to increase the electrical signal level.

B. Continuous Periodic Millimeter Waveform Generation

The preceding section details the generation of arbitrarily phase- and frequency-modulated burst waveforms in the multiple-tens-of-gigahertz range. The burst nature of these waveforms is determined by the laser source used as the input to our system. Thus far, our waveforms span a time aperture in excess of 100 ps and repeat at the source repetition rate of 40 MHz, so they are essentially isolated in time. For applications requiring higher data rates, it is desirable to have waveforms that are con-

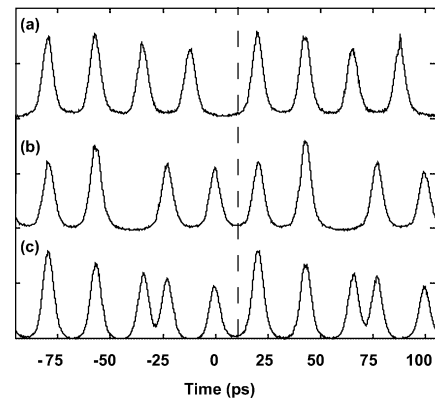


Fig. 9. Optical cross-correlation traces of ~ 40 -GHz optical pulse sequences used to generate nearly continuous electrical waveforms. Each frame of pulses (separated by the dashed line) is generated from a single source pulse every 100 ps. (a) 40-GHz periodic sequence. (b) 40-GHz sequence with an extra ~ 12.5 -ps delay introduced after the second pulse in each frame. (c) 40-GHz sequence with an 80-GHz pulse pair introduced following the second pulse.

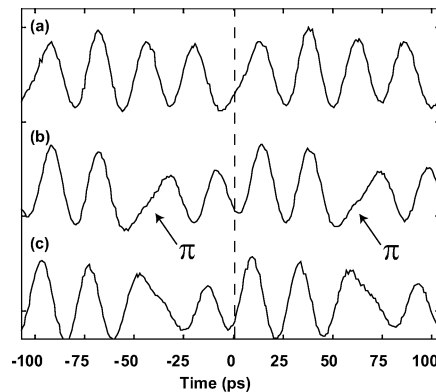


Fig. 10. Electrical waveforms resulting from O/E conversion of the pulse sequences of Fig. 9. (a) Nearly continuous 40-GHz sinusoid. (b) 40-GHz phase-modulated waveform exhibiting a π phase shift after the second cycle in each frame. (c) Modulated waveform showing a phase shift midway through the third cycle.

tinuous in nature, i.e., shaped electromagnetic waveforms that repeat at a period approaching the pulse shaping window.

To move toward generation of such waveforms, we have replaced the passively mode-locked fiber laser with an actively mode-locked fiber source [15] that provides ~ 1 -ps pulses at a repetition rate of 10 GHz. The goal here is to combine our ability to generate electromagnetic waveforms over a ~ 100 -ps frame with a source of comparable pulse period to generate continuous millimeter waveforms. The idea is to create an arbitrarily shaped millimeter waveform, spanning this frame, from each source pulse and then stitch these waveforms together to form a continuous signal. To illustrate this concept, consider Figs. 9 and 10. Here, the pulse sequences of Fig. 9 generate the electrical waveforms of Fig. 10 after O/E conversion.

In Fig. 9(a), a frame consisting of four pulses at ~ 40 GHz is generated in the DST shaper from each pulse from the source. The dashed line delineates the boundary between adjacent frames. After O/E conversion, the ~ 40 -GHz electrical waveform of Fig. 10(a) results. Similarly, the phase-modulated waveforms of Fig. 10(b) and (c) are generated from the pulse sequences of Fig. 9(b) and (c). In (b), an extra ~ 12.5 -ps delay is added after the second pulse in the driving optical pulse sequence. This extra delay results in a π phase shift following

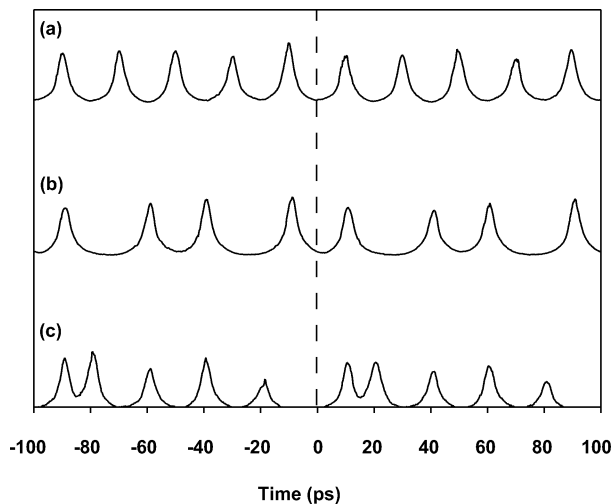


Fig. 11. Driving optical pulse sequences used to generate continuous millimeter waveforms. (a) 50-GHz optical pulse sequence. (b) Pulse sequence exhibiting an extra 10-ps delay after the first and third pulse in each frame. (c) 100-GHz pulse pair followed by three pulses at 50 GHz, which repeats every 100 ps.

the second cycle of the electrical waveform. Similarly, the shift in (c) is generated by driving the third electrical cycle with a single 80-GHz pulse pair. The concept of stitching together frames is clearly demonstrated here; however, the need to match the waveform duration and the source repetition rate is also illustrated. If we wish to achieve continuous waveforms, the pulse sequence duration from the DST shaper and, hence, the duration of the electrical waveform must be chosen such that the frames join appropriately at the frame boundary. For example, consider the pulse sequence and electrical waveform of (a). There is an obvious stitching error at the frame boundary that results from a mismatch in frame duration and the source pulse period. This leads to a small phase shift at the frame boundary in the electrical waveform. To match the electrical waveforms at the frame boundaries and remove this error, the duration of the driving optical pulse sequence must be chosen appropriately. To change the duration of the optical pulse sequence, we simply change the periodic spatial pattern applied to the pulse shaper input. One proper choice of spatial pattern leads to a pulse sequence from the DST where the pulse-to-pulse spacing is 20 ps, and the frame duration is 100 ps, resulting in a continuous 50-GHz optical pulse sequence with negligible stitching error between adjacent frames. This continuous pulse sequence is illustrated in Fig. 11(a). After O/E conversion, the measured electrical waveform is seen to be a smooth ~ 50 -GHz sinusoid, as illustrated in Fig. 12(a). Here, the stitching error apparent in Fig. 10(a) has been effectively eliminated.

We are also able to achieve phase and frequency modulation (FM) in the same manner as previously demonstrated with burst waveforms. For example, an extra 10-ps delay is introduced after the first and third pulses in the optical pulse sequence of Fig. 11(b), which results in a 50-GHz sinusoid exhibiting a π phase shift after the first and third cycles in the electrical waveform [Fig. 12(b)]. Similarly, by introducing a single ~ 100 -GHz pulse pair [Fig. 11(c)], a single 25-GHz cycle precedes three 50-GHz cycles, as shown in Fig. 12(c).

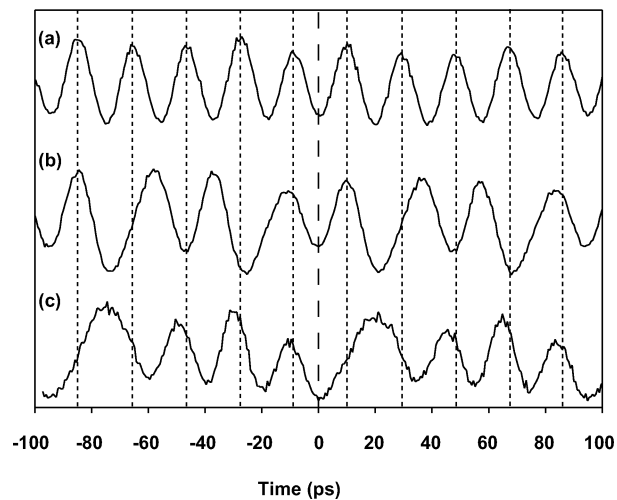


Fig. 12. Continuous millimeter waveforms. Individual waveforms, spanning a 100-ps frame as delineated by the dashed line, are stitched together to form continuously periodic millimeter waveforms. (a) Continuous 50-GHz sinusoid. (b) Periodically phase-modulated waveform exhibiting a π phase shift after the first and third electrical cycles within each frame. (c) 25/50-GHz frequency-modulated waveform. A single 25-GHz cycle is induced by a 100-GHz pulse pair [Fig. 11(c)] followed by three ~ 50 -GHz cycles.

By matching the ability to form optical pulse sequences over a time aperture ≥ 100 ps with a high-repetition-rate source, we are able to generate continuous arbitrary electromagnetic waveforms at center frequencies of ~ 50 GHz. These waveforms, due to increased optical excitation power, exhibit peak-to-peak amplitudes of approximately 20 mV. Again, wide-band electronic amplification or a further increase in optical excitation could be used to increase the amplitudes of these signals. We note the modulation is arbitrary within one frame and is repeated at the source repetition rate. Incorporation of a high-speed optoelectronic modulator array for rapid reprogramming of the spatial pattern at the input of the DST pulse shaper would allow reprogramming of the optical pulse sequences on a frame-by-frame basis. This ability would allow generation of arbitrarily shaped millimeter waveforms where the modulation varies independently from frame to frame.

IV. GENERATION OF GIGAHERTZ WAVEFORMS VIA DST PULSE SHAPING AND DISPERSIVE STRETCHING

For certain applications, particularly ultra-wide-band RF communications [5], it is desirable to obtain arbitrarily shaped electromagnetic waveforms in the gigahertz range. Given the February 2002 ruling by the Federal Communications Commission (FCC), a particular frequency range of interest is the approved UWB 3.1–10.6 GHz band. Keeping in mind the goal of reaching this particular frequency range, we now show how to move our electromagnetic waveform generation technique from the tens-of-gigahertz range into the gigahertz range.

While both FT and DST pulse shaping techniques are capable of generating optical waveforms that span a time aperture of several hundred picoseconds, achieving waveforms with nanosecond durations directly from either pulse shaper is not feasible. Inclusion of a fixed amount of chromatic dispersion after either shaper, however, can easily stretch the temporal durations into the nanosecond regime. Recently, a group at the Uni-

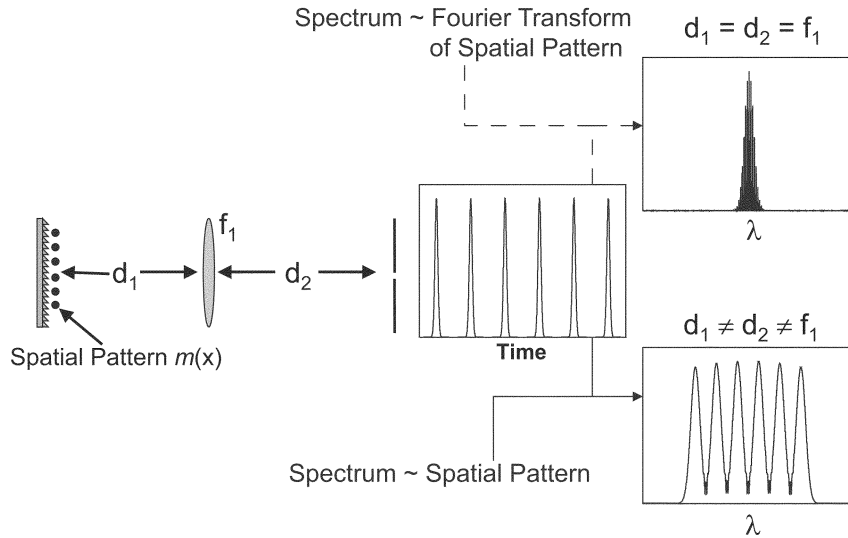


Fig. 13. FM in the DST shaper. A quadratic temporal phase is imparted to the pulse shaper output when $d_1, d_2 \neq f_1$. For a sufficiently large FM, the applied spatial pattern is mapped to the optical spectrum at the output of the DST shaper. This FM capability, combined with dispersive stretching, allows the ~ 100 -ps optical pulse sequences from the DST to be stretched to several nanoseconds in duration.

versity of California at Los Angeles (UCLA) [9] demonstrated a Fourier pulse-shaping technique, combined with dispersive stretching, to generate RF waveforms in the 1–12-GHz range. In this method, the optical spectrum of a supercontinuum source is amplitude-modulated in an FT pulse shaper [13]. Following the pulse shaper, a length of single-mode optical fiber dispersively stretches the temporal output of the pulse shaper. For large dispersion, the measured optical waveform after stretching is a scaled version of the amplitude modulation applied to the optical spectrum. This is equivalent to the Fourier transform of the pulse shaper temporal output. After O/E conversion, the measured temporal electrical waveform exhibits the shape of the optical spectrum.

While conceptually similar, the fundamental difference between the FT technique [9] and our DST shaping technique is the manner by which the optical spectrum is modulated and the relation between the pulse shaper temporal output and the measured electrical waveform. In contrast to direct modulation of the optical spectrum via an SLM in an FT shaper, the optical spectrum in our apparatus is modulated by the applied spatial pattern and the physics of the DST pulse shaping apparatus.

In a DST pulse shaper, the intensity of the output temporal waveform is always a scaled version of the applied spatial pattern, as given by (1). It has been shown, however, that a quadratic temporal phase may be imparted to the DST shaper temporal output when the apparatus is configured appropriately [16]. To illustrate this concept, consider Fig. 13. If we assume a perfectly collimated spatial input to the pulse shaper, the apparatus contributes no quadratic spatial phase when configured in a “chirp-free,” i.e., $d_1 = d_2 = f_1$, configuration. In this particular case, the phase fronts of both the spatial pattern applied to the grating and the spectrum prior to the output fiber are flat, and the DST shaper does not impart any quadratic phase or FM to the temporal output waveform. The result is that the optical spectrum of the pulse shaper output is related to the Fourier transform of the temporal output as is expected. When the pulse shaping lens is moved from the chirp-free position, i.e.,

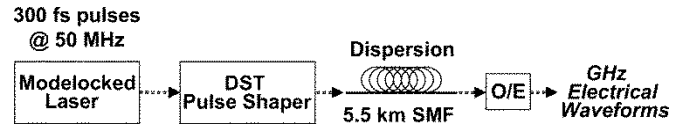


Fig. 14. Experimental schematic for gigahertz waveform generation. Optical pulse sequences from the DST shaper are temporally stretched by ~ 5.5 km of single-mode optical fiber prior to O/E conversion, enabling generation of electrical waveforms spanning several nanoseconds.

$d_1 \neq d_2 \neq f_1$, however, the phase front at the output fiber now has a curvature and, hence, a quadratic spatial phase. Through the physics of the pulse shaper, this quadratic spatial phase maps to a quadratic temporal phase in the DST output, which is now expressed as

$$E_{\text{DST}}(t) \propto e_{\text{in}}(t) * \left[m \left(-\frac{\alpha}{\gamma} t \right) e^{-jAt^2} \right] \quad (3)$$

where

$$A(d_1, d_2) = \frac{\pi}{\lambda\gamma^2} \left(\frac{f_1 - d_2}{f_1 d_1 + f_1 d_2 - d_1 d_2} \right). \quad (4)$$

This quadratic temporal phase gives rise to an FM (in nanometers per picosecond) which, when sufficiently large, maps the applied spatial pattern onto the optical spectrum. In this case, both the temporal waveform and the optical spectrum are scaled versions of the applied spatial pattern. Thus, when the DST shaper is followed by a fixed amount of dispersion, as illustrated in Fig. 14, the optical waveform after stretching is still a directly scaled version of the pulse shaper temporal output. After O/E conversion, the electrical waveform is now a stretched version of the pulse shaper output.

The stretching factor is determined by the magnitude of FM imparted by the pulse shaper and the amount of fixed dispersion. For our system, which employs $L \sim 5.5$ km of Corning SMF-28 ($D = 17$ ps/nm-km), the stretching factor is approximately given by

$$\text{Stretching Factor} \sim |\text{FM}| \cdot D \cdot L. \quad (5)$$

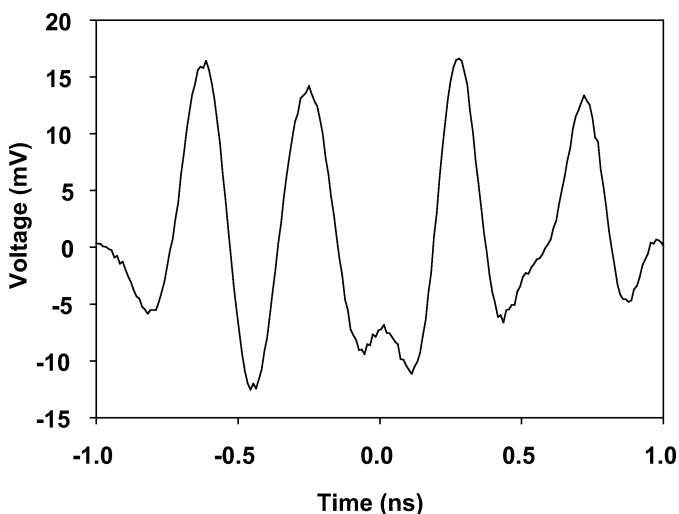


Fig. 15. Gigahertz waveform generation. After passing through ~ 5.5 km SMF, the ~ 70 ps four-pulse 50-GHz sequence from the DST shaper is stretched ~ 20 times. After O/E conversion, the measured four-cycle electrical waveform has a duration of ~ 1.34 ns and a center frequency of ~ 2.6 GHz.

In our apparatus, a variety of stretching factors are attainable. As the pulse-shaping lens is displaced from the chirp-free position of $d_1 = 15$ cm = f_1 to $d_1 = 11.25$ cm, the induced FM is continuously tuned from 0 to -0.3 nm/ps. This variation in chirp gives a stretching factor that varies from 0 \sim 28 over this small range of lens position.

It is interesting to compare our gigahertz waveform generation concept with that of temporal imaging [17]. Temporal imaging is accomplished through the combination of dispersion, quadratic temporal phase modulation, and a second dispersion applied to an input optical waveform [18]. When the dispersion and phase modulation are chosen appropriately, the input optical waveform is mapped to an output waveform that is either temporally expanded or compressed. The key element in these systems is the quadratic phase modulator, or time lens [19]. Although our system is not configured in an exact imaging geometry, our DST shaper operates as just such a lens—where the temporal focal length is easily tuned through longitudinal displacement of the pulse-shaping lens.

We now present several examples of gigahertz waveform generation in our system. As a first example, the DST lens is positioned to give an FM of ~ -0.22 nm/ps, yielding a predicted stretching factor of ~ 20.57 . Experimentally, when a four-pulse sequence that is 70 ps in duration and has a center frequency of ~ 50 GHz is generated in the DST shaper, the measured stretched electrical waveform is found to have a duration of ~ 1.34 ns to approximately 20 times the duration of the initial waveform. This waveform is presented in Fig. 15.

The duration of the measured waveform shows excellent agreement with the predicted duration, with the slight discrepancy most likely due to uncertainty in the length of the stretching fiber.

For a fixed amount of dispersion, in our case $D \cdot L \approx 93.5$ ps/nm, the stretching factor may be tuned simply by changing the position of the pulse-shaping lens. For small changes in lens position, $\pm 10\%$ changes in temporal duration are easily attainable. To illustrate this tunability of the electrical waveform duration, a four-pulse 100-ps pulse sequence is

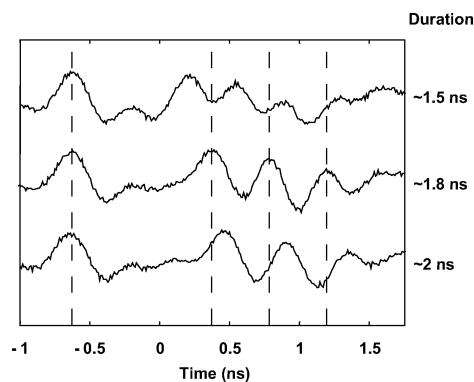


Fig. 16. Tunability of electrical waveform duration. For small changes in pulse-shaping lens position, $\pm 10\%$ changes in waveform duration are easily attained. Here, the electrical waveform is scaled from 1.5–2 ns, amounting to a center frequency variation over the range of ~ 3.33 –2.5 GHz, for a change in lens position of 7.5 mm.

generated in the DST shaper. This sequence can be represented as “1 0 0 1 1 1”, with “1” representing a pulse in the sequence. In this sequence, each pulse occupies a 20-ps frame, resulting in a center frequency of ~ 50 GHz. This waveform, after stretching and O/E conversion, is shown for several stretching factors in Fig. 16. The center waveform, exhibiting a duration of ~ 1.8 ns, as measured from the separation of the first and last peak in the waveform, will be used as the reference. Dividing this sequence duration into five 360-ps frames, the waveform exhibits a center frequency of ~ 2.77 GHz. To achieve this waveform, the pulse-shaping lens is positioned with $d_1 = 13.25$ cm and $d_2 = 16.75$ cm (please see Fig. 13), resulting in an FM of ~ -0.20 nm/ps in the pulse shaper. For this value of FM, the predicted stretching factor as given by (5) is approximately 18.7. The measured ~ 1.8 -ns waveform shows excellent agreement with this predicted value. By repositioning the pulse-shaping lens, this waveform may be contracted or dilated in time. For example, when the pulse-shaping lens is positioned 5 mm from the reference position ($d_1 = 13.75$ cm, $d_2 = 16.25$ cm), the top electrical waveform results. The waveform is contracted from 1.8 to approximately 1.5 ns, which again shows excellent agreement with the predicted duration of ~ 1.49 ns. Again dividing the waveform duration into five equal frames, this waveform exhibits a ~ 3.33 -GHz center frequency. To dilate the waveform, the lens is displaced -2.5 mm from the reference position ($d_1 = 13$ cm, $d_2 = 17$ cm). In this position, the applied FM increases in magnitude to approximately -0.22 nm/ps, yielding a stretching factor of ~ 20.5 . The measured ~ 2 ns (~ 2.5 GHz) electrical waveform is shown in the bottom trace. Although we focus on time-domain waveforms here, it should be noted that the entire broad-band RF spectrum is, in fact, tuned in frequency space. This clearly illustrates how, through very small adjustments to the pulse shaper, the temporal duration and broad-band RF spectrum of arbitrarily shaped waveforms can easily be tuned over a range greater than $\pm 10\%$.

V. CONCLUSION

We present an overview of our novel optical technique for generation of arbitrarily shaped broad-band electromagnetic waveforms in the gigahertz-to-multiple-tens-of-gigahertz

range. By using tailored optical pulse sequences generated in a novel DST optical pulse shaper to drive a high-speed photodiode, we generate amplitude-equalized arbitrarily phase- and frequency-modulated waveforms. This technique, which allows generation of electrical waveforms at center frequencies approaching 50 GHz, is extended to generation of waveforms in the gigahertz range through dispersive stretching of the pulse shaper output. This simple technique for millimeter and microwave AWG could be an enabling technology for a variety of applications, including RF communications, pulsed radar, and fiber-wireless communication systems.

REFERENCES

- [1] J. C. Twichell, J. L. Wasserman, P. W. Juodawlkis, G. E. Betts, and R. C. Williamson, "High-linearity 208-ms/s photonic analog-to-digital converter using 1-to-4 optical time-division demultiplexers," *IEEE Photon. Technol. Lett.*, vol. 13, pp. 714–716, July 2001.
 - [2] T. R. Clark and M. L. Dennis, "Toward a 100-gsample/s photonic a-d converter," *IEEE Photon. Technol. Lett.*, vol. 13, pp. 236–238, Mar. 2001.
 - [3] A. S. Bhusan, P. V. Kelkar, B. O. Boyraz, and M. Islam, "130-gsa/s photonic analog-to-digital converter with time stretch preprocessor," *IEEE Photon. Technol. Lett.*, vol. 14, pp. 684–686, May 2002.
 - [4] C. Lim, A. Nirmalathas, D. Novak, R. Waterhouse, and G. Yoffe, "Millimeter-wave broad-band fiber-wireless system incorporating baseband data transmission over fiber and remote lo delivery," *J. Lightwave Technol.*, vol. 18, pp. 1355–1363, Oct. 2000.
 - [5] M. Z. Win and R. A. Scholtz, "Ultra-wide bandwidth time-hopping spread-spectrum impulse radio for wireless multiple-access communications," *IEEE Trans. Commun.*, vol. 48, pp. 679–691, Apr. 2000.
 - [6] S. Poinsot, H. Porte, J.-P. Goedgebuer, W. T. Rhodes, and B. Boussert, "Continuous radio-frequency tuning of an optoelectronic oscillator with dispersive feedback," *Opt. Lett.*, vol. 27, pp. 1300–1302, 2002.
 - [7] T. Yilmaz, C. M. DePriest, T. Turpin, J. H. Abeles, and P. J. Delfyett, "Toward a photonic arbitrary waveform generator using a modelocked external cavity semiconductor laser," *IEEE Photon. Technol. Lett.*, vol. 14, pp. 1608–1610, Nov. 2002.
 - [8] B. Jalai, P. Kelkar, and V. Saxena, "Photonic arbitrary waveform generator," in *Proc. 14th Annu. Meeting IEEE*, vol. 1, Nov. 2001.
 - [9] J. Chou, Y. Han, and B. Jalai, "Adaptive RF-photonic arbitrary waveform generator," *IEEE Photon. Technol. Lett.*, vol. 15, pp. 581–583, Apr. 2003.
 - [10] D. E. Leaird and A. M. Weiner, "Femtosecond direct space-to-time pulse shaping," *IEEE J. Quantum Electron.*, vol. 37, pp. 494–504, Apr. 2001.
 - [11] J. D. McKinney, D. E. Leaird, and A. M. Weiner, "Millimeter-wave arbitrary waveform generation with a direct space-to-time pulse shaper," *Opt. Lett.*, vol. 27, pp. 1345–1347, 2002.
 - [12] J. D. McKinney, D. S. Seo, and A. M. Weiner, "Photonic assisted generation of continuous arbitrary millimeter electromagnetic waveforms," *Electron. Lett.*, vol. 39, pp. 309–311, 2003.
 - [13] A. M. Weiner, "Femtosecond pulse shaping using spatial light modulators," *Rev. Sci. Instrum.*, vol. 71, p. 1929, 2000.
 - [14] D. E. Leaird and A. M. Weiner, "Femtosecond optical packet generation by a direct space-to-time pulse shaper," *Opt. Lett.*, vol. 24, pp. 853–855, 1999.
 - [15] T. F. Carruthers and I. N. Duling III, "10-GHz, 1.3-ps erbium fiber laser employing soliton pulse shortening," *Opt. Lett.*, vol. 21, pp. 1927–1929, 1996.
 - [16] D. E. Leaird and A. M. Weiner, "Chirp control in the direct space-to-time pulse shaper," *Opt. Lett.*, vol. 25, pp. 850–852, 2000.
 - [17] C. V. Bennet and B. H. Kolner, "Upconversion time microscope demonstrating $103\times$ magnification of femtosecond waveforms," *Opt. Lett.*, vol. 24, pp. 783–785, 1999.
 - [18] B. H. Kolner and M. Nazarathy, "Temporal imaging with a time lens," *Opt. Lett.*, vol. 14, pp. 630–632, 1989.
 - [19] B. H. Kolner, "Generalization of the concepts of focal length and f-number to space and time," *J. Opt. Soc. Amer. A*, vol. 11, pp. 3229–3234, 1994.
- Jason D. McKinney** (M'03) received the Ph.D. degree from the School of Electrical and Computer Engineering, Purdue University, West Lafayette, IN, in 2003.
- From July 2001 through May 2003, he was a Graduate Assistance in Areas of National Need (GAANN) Fellow sponsored by the U.S. Department of Education. He is currently a Visiting Assistant Professor of Electrical and Computer Engineering at Purdue University. His research focuses on the area of optical space-time processing and radio frequency photonics—specifically, optical pulse shaping for arbitrary electromagnetic waveform generation.
- Dr. McKinney was a finalist for the Optical Society of America (OSA)/New Focus Student Award in 2002, and in 2003, he received the Chorafas prize for outstanding doctoral research from the Dimitris N. Chorafas Foundation, as well as the Motorola Student Excellence Award for academic merit and leadership. He has also received numerous awards in recognition of his teaching ability and is an Associate Fellow of the Purdue University Teaching Academy. He is a Member of the Optical Society of America (OSA).
- Dongsun Seo**, photograph and biography not available at the time of publication.
- Daniel E. Leaird** (M'01), photograph and biography not available at the time of publication.
- Andrew M. Weiner** (S'84–M'84–SM'91–F'95) received Sc.D. degree in electrical engineering from the Massachusetts Institute of Technology (MIT), Cambridge, in 1984.
- From 1979 through 1984, he was a Fannie and John Hertz Foundation Graduate Fellow at MIT. In 1984, he joined Bellcore, which at that time, was one of the premier research organizations in the telecommunications industry. In 1989, he was promoted to Manager of Ultrafast Optics and Optical Signal Processing. In 1992, he joined Purdue University, West Lafayette, IN, as Professor of Electrical and Computer Engineering (ECE) and is currently the Scifres Distinguished Professor of Electrical and Computer Engineering. From 1997 to 2003, he also served as ECE Director of Graduate Admissions. He has published four book chapters and more than 120 journal articles. He has been author or coauthor of more than 200 conference papers, including approximately 60 conference invited talks, and has presented more than 50 additional invited seminars at universities or industry. He has also served as an Associate Editor of *Optics Letters*. He is holder of five U.S. patents. His research focuses on ultrafast optical signal processing and high-speed optical communications, and he is especially well known for pioneering the field of femtosecond pulse shaping, which enables generation of nearly arbitrary ultrafast optical waveforms according to user specifications.
- Prof. Weiner is a Fellow of the Optical Society of America. He has received numerous awards for his research, including the Hertz Foundation Doctoral Thesis Prize (1984); the Adolph Lomb Medal of the Optical Society of America (1990), awarded for pioneering contributions to the field of optics made before the age of 30; the Curtis McGraw Research Award of the American Society of Engineering Education (1997); the International Commission on Optics Prize (1997); the IEEE Lasers & Electro-Optics Society (LEOS) William Streifer Scientific Achievement Award (1999); the Alexander von Humboldt Foundation Research Award for Senior U.S. Scientists (2000); and the inaugural Research Excellence Award from the Schools of Engineering at Purdue (2003). He has served on or chaired numerous research review panels, professional society award committees, and conference program committees. In 1988–1989, he served as an IEEE LEOS Distinguished Lecturer. He was General Co-Chair of the 1998 Conference on Lasers and Electro-Optics, Chair of the 1999 Gordon Conference on Nonlinear Optics and Lasers, and Program Co-Chair of the 2002 International Conference on Ultrafast Phenomena. In addition, he has served as Associate Editor for the IEEE JOURNAL OF QUANTUM ELECTRONICS and the IEEE PHOTONICS TECHNOLOGY LETTERS. He has also served as an Elected Member of the Board of Governors of IEEE LEOS from 1997–1999 and as Secretary/Treasurer of IEEE LEOS from 2000–2002. He is currently a Vice-President (representing IEEE LEOS) of the International Commission on Optics (ICO).